ELSEVIER

Polymer 40 (1999) 7117–7124

polymer

Characterization of amorphous domains in cellulosic materials using a FTIR deuteration monitoring analysis

Y. Hishikawa, E. Togawa, Y. Kataoka, T. Kondo*

Forestry and Forest Products Research Institute (FFPRI), P.O. Box 16, Tsukuba Norin Kenkyu, Tsukuba-city, Ibaraki 305-8687, Japan

Received 4 June 1998; received in revised form 8 December 1998; accepted 28 January 1999

Abstract

We have attempted to develop a technique to characterize the amorphous or non-crystalline regions in cellulosic materials using Fourier transform infra-red spectroscopy to monitor the deuteration process for a film sample, followed by a subsequent kinetic analysis. It is possible that the H–D exchange reaction rate for OH groups in the films may reveal the nature or extent of the amorphous regions. The morphological contribution of the film surface to the analysis was determined using atomic force microscopy for both cast and coagulated cellulose films. The results showed that the surface of cast films are much rougher than that of coagulated ones. However, during the initial 5 min of the deuteration process, both types of films gave similar values for the D_2O diffusion coefficient, indicating that the differences in the cellulose film surfaces did not have a significant effect on the D_2O penetration diffusion rate. Next we examined whether the OH–OD exchanging rate, which was found to exhibit pseudo-first-order kinetics, could or could not be used to comment on the nature or extent of amorphous regions present in the films. We also examined the relationship, if any, between the exchange rate and the diffusion coefficient. Other amorphous cellulosic films, composed of regioselectively methylated cellulose, such as 2,3-di-*O*-methylcellulose (23MC) and 6-*O*-methylcellulose (6MC) were also studied and the results were compared with the cast and coagulated films of pure cellulose. The results indicated that the non-crystalline phase of cellulosic films are not composed solely of homogeneous domains nor are they totally amorphous but rather they were found to have a heterogeneous organization.

Keywords: Cellulose; Methylcelluloses; Amorphous regions

1. Introduction

There is a notable lack of structural information about the amorphous or non-crystalline regions of cellulose when compared with the abundance of information available on the crystalline regions. This may, perhaps be partly because the terminology suggests and the impression persists that molecular chains in the amorphous regions are completely without structure, and partly because the methodology has been limited to WAXD and CP-MAS ^{13}C NMR for measuring order in the presence of substantial amounts of disorder [1]. It is not uncommon for substrates, which are not crystalline to be classified by a method such as X-ray diffraction, to be labeled "amorphous" but the true definition of amorphous goes beyond merely non-crystalline and really refers to unorganized and having no pattern or structure [2]. Our objective is to focus on the amorphous or non-crystalline regions of cellulose and to characterize these regions using a deuteration method combined with Fourier transform infrared (FTIR) spectroscopic measurements to monitor continually the deuteration process in the sample, followed by a subsequent kinetic analysis.

Mann has reported [3] that combining the D_2O-deuteration of cellulose with infrared (IR) spectroscopy leads to the development of a unique tool to structurally study cellulose. This is true because rapid conversion of hydroxyl (OH) groups into deuterated (OD) groups by D_2O or D_2O vapor in the amorphous regions results in distinct amorphous and crystalline regions in the IR spectrum for the supermolecular structure of cellulose. In fact, in structural studies undertaken by some researchers the goal was to separate the cellulose structure into ordered and disordered regions and thus to determine the accessibility value for cellulose [4–8]. The structure of the crystalline regions was also investigated mainly because the almost perfect crystalline regions were very suitable for studying their structures alone without any contributions from the amorphous regions [7,9–11]. The amorphous regions were almost totally neglected by these researchers who used the combination of deuteration and FTIR spectroscopy. Recently, we have discussed the utility

* Corresponding author. Tel.: + 81-298-73-3211-531; fax: + 81-298-73-3797.

E-mail address: kondot@ss.ffpri.affrc.go.jp (T. Kondo)

0032-3861/99/$ - see front matter
PII: S0032-3861(99)00120-2

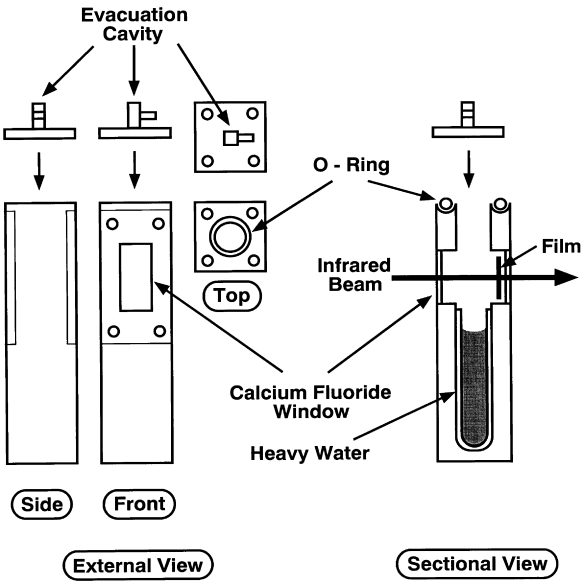

Fig. 1. A modified IR absorption cell for monitoring the deuteration process.

of the aforementioned method to characterize the nature of the amorphous phase in cellulose [1]. In this article, we have investigated the contribution of morphological differences in the film surface to the FTIR-deuteration monitoring analysis using both cast and coagulated cellulose films having totally different morphologies.

2. Experimental

2.1. Preparation of cast and coagulated cellulose films

Two types of cellulose films were prepared from dimethylacetamide/lithium chloride (DMAc-LiCl) cellulose solution [12]. Cast cellulose film [13] exhibited a crystallinity index (Cr.I.) of 0.0%, whereas a coagulated cellulose film had a Cr.I. of 13.8%, determined by X-ray analyses. The latter film was obtained by slow coagulation of the DMAc-LiCl cellulose solution under saturated water vapor followed by subsequent water-washing and drying under vacuum at room temperature [14]. Each preparation method resulted in a film with a thickness of 5 μm. The two films were then dried thoroughly in a vacuum oven at 50°C in order to remove all residual water prior to deuteration.

2.2. Measurements

An air-side or top surface of each film was observed in a Digital Instruments NanoScope IIIa atomic force microscope (AFM) in tapping mode using a scan rate of 0.5–2 Hz. FTIR spectra were recorded using a Perkin–Elmer Spectrum 2000 FTIR spectrometer or a Nicolet Magna-IR spectometer 550 FTIR spectrometer using a special IR absorption cell (described later) for deuteration. The parameters for the IR measurements were as follows: six scans for the Perkin–Elmer Spectrum 2000 or 34 scans for the Nicolet Magna-IR 550 spectometer with a 2 cm^{-1} resolution (scanning time for both was 69 s), a DTGS detector and the wavenumber region investigated ranged from 4000 to 400 cm^{-1}. Spectra were recorded continually until the OH–OD exchange reaction reached an equilibrium state.

2.3. Special IR absorption cell to monitor the deuteration process

A modified IR absorption cell (Fig. 1) was required to monitor the deuteration process. The cell consists of two calcium fluoride windows, a D_2O reservoir inside, and a cavity, for evacuation on the top, which is sealed with an O-ring. A large amount of D_2O (the purity was more than 99.75%) was poured into the reservoir after a completely dried film sample was placed inside the cell so it rested on the rear window so that the deuteration could proceed only from the air-side surface of the film. The cell was then tightly closed and evacuated so that the sample cell would be completely saturated with D_2O vapor. The cell was then quickly put into the sample compartment of the FTIR spectrometer and spectra were recorded as a function of time at 25°C.

3. Results and discussion

3.1. AFM observation of the surface morphology for the cellulose films

Fig. 2 shows the surface morphology for the two types of cellulose films and their cross sectional profiles; (A) is the cast film, (B) is the coagulated film, and (C) and (D) are enlargements of the same surfaces for the cast (an enlargement of the square in (A)) and for the coagulated film, respectively. In both the illustrated film areas ((A) and (B)) of 60.0 μm × 60.0 μm, the surface morphologies were significantly different from each other. The cast film surface was much rougher than the smooth surface of the coagulated film. In particular, the enlarged image of the coagulated cellulose film revealed that the surface (D) of the film was much more porous than that of the cast film (C). In comparing the size of holes in the cross sectional profiles of films (C) and (D), the largest hole found in the cast film was about 1000 nm in diameter and about 100 nm in depth whereas for the coagulated film the corresponding values were about 200 nm and about 30 nm, respectively. Unfortunately, further enlargement to a few nm level, which would be close to the size of D_2O, was impossible. We did, however, find direct evidence that the surface morphologies of cellulose films are influenced by their preparation method. During the film casting method, the solvent in DMAc-LiCl cellulose solution was evaporated rapidly and, therefore, many large holes remain on the surface as

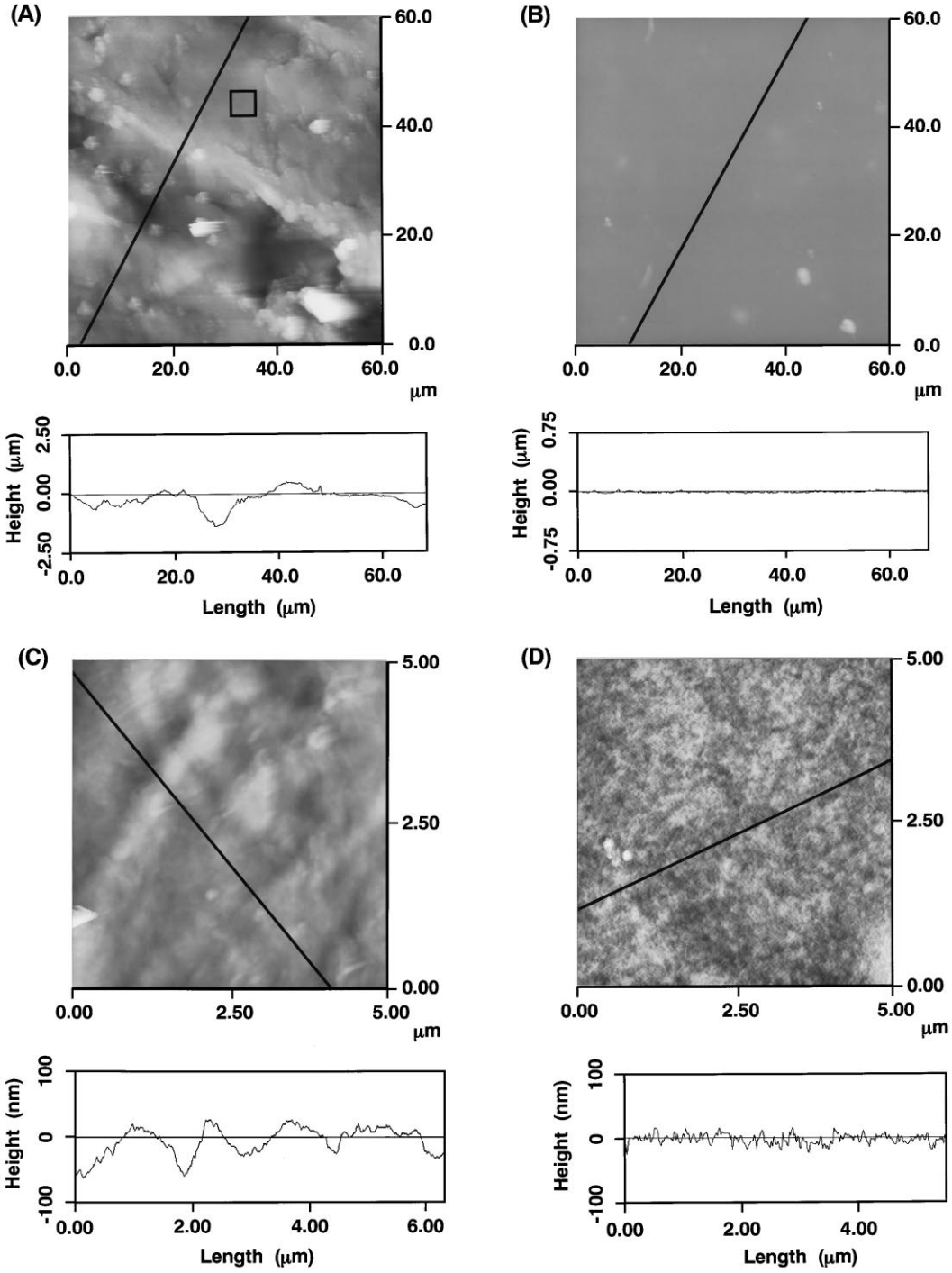

Fig. 2. AFM micrographs of the surface morphology for the cellulose films (above) and their corresponding profiles (below): (A) cast film; (B) coagulated film; (C) an enlargement of the same surface for the cast film; (D) and for the coagulated film.

evidence of fast removal of solvent molecules. In contrast in the film coagulation method, the β-glucan molecules can self-organize and aggregate slowly in water vapor to form the cellulose film by a subsequent water-washing in which the solvent was gradually removed from the coagulated gel of the solution. Therefore, holes on the surface of coagulated films are much smaller than those found in cast films.

3.2. IR spectra of films during deuteration with D_2O vapor

Fig. 3 shows the change in IR spectra for a cast cellulose film during the deuteration process. While the intensity of the OH absorption band at 3415 cm^{-1} due to stretching of the OH groups decreased during deuteration, the absorption band at 2515 cm^{-1} due to stretching of OD groups appeared

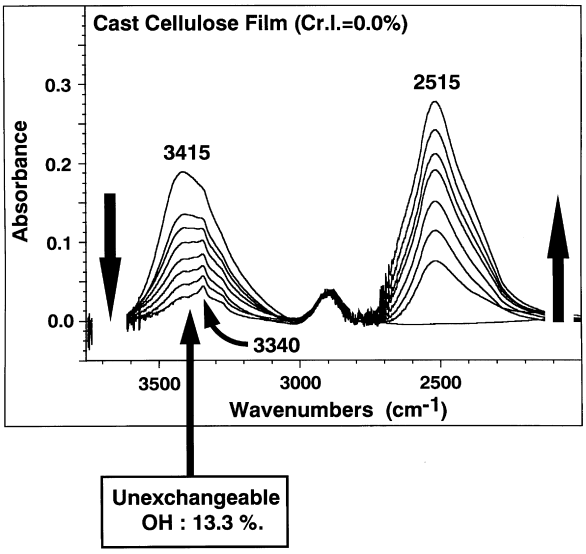

Fig. 3. Changes in OH and OD IR absorption bands with time during the deuteration process with D_2O vapor for cast cellulose film (Crystallinity Index: Cr.I. = 0.0%).

and increased with the deuteration process. Similar behavior was obtained for the coagulated cellulose film as exhibited in Fig. 4. These data indicate that OH groups are almost equivalently exchanged into OD groups during the deuteration process under a saturated atmosphere of D_2O vapor.

With further deuteration, the reaction reaches an equilibrium value. In such an equilibrium state, the absorption band for OH groups at 3340 cm^{-1} for the cast film and at 3427 cm^{-1} for the coagulated film, respectively (Figs. 3 and 4), still remain. This remaining OH band for the amorphous cast film indicates the existence of unreacted OH groups. Mann and Marrinan reported previously [4] that the OH groups in the amorphous regions of cellulose were

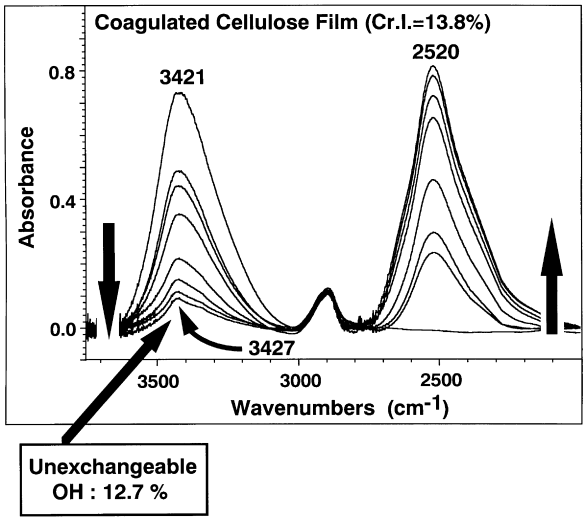

Fig. 4. Changes in OH and OD IR absorption bands with time during the deuteration process with D_2O vapor for coagulated cellulose film (Cr.I. = 13.8%).

thoroughly deuterated by D_2O vapor at room temperature. However, the OH groups in our cast cellulose film (Cr.I.: 0.0%), which exhibits amorphous character in the X-ray diffraction pattern, were not completely deuterated, and the amount of unexchangeable OH groups was 13.3% of the total OH groups. Similar results were reported by Wadehra et al. [15] and Jeffries [16]. They explained the existence of unreacted OH groups in amorphous cellulose as being due to a small amount of recrystallized domains being present during the accessibility measurement at 100% relative humidity of D_2O vapor. Further, Wadehra et al. reported that the recrystallization occurred during the initial 4 h judging from changes in the X-ray diffraction patterns [15]. However, our kinetic analysis for the three types of amorphous cellulosic samples (the cast cellulose film, the cast 2,3-di-*O*-methylcellulose film and the cast 6-*O*-methylcellulose film) never showed any recrystallization in the saturated D_2O vapor. If such recrystallization occurs during the initial stage, each reaction rate for the aforementioned three films would not be kept constant because the D_2O vapor should be wasted not only for the OH–OD exchange as a pseudo-first-order kinetic reaction but also for induction of the recrystallization. In addition, the IR band shape for the OH stretching frequencies should have been changed with the crystalline formation in the cellulosic films. In fact, such phenomena, however, were not found in our systems for the aforementioned three samples (see Figs. 7 and 3, and Ref. [1]). Therefore, we have assumed that this unexchangeable OH band indicates the presence of intermolecular hydrogen-bonded domains which had been formed in the amorphous regions when the film was prepared. This supermolecular structure has been already proposed for a model [13] of the amorphous regions. In those domains, the β-glucan molecules appear to be held together by intermolecular hydrogen bonds to an extent great enough to prevent the penetration of D_2O molecules, but not so tightly as those found in crystalline regions. We have also assumed that the unexchangeable OH groups in the coagulated cellulose film (12.7% of the total OH groups) were made up of OH groups in both hydrogen-bonded domains or microcrystallites and the crystalline regions. A more detailed characterization of the nature of the amorphous regions in cellulose will be presented in the following section (Section 3.3) from the view point of a kinetic analysis of the OH–OD exchange.

3.3. Kinetic analysis of OH–OD exchange

The OH–OD exchange in the amorphous regions for both films was kinetically analyzed by monitoring the behavior of (1) the OD band increase (D_2O diffusion) and (2) the OH band reduction (deuteration of OH).

3.3.1. D_2O diffusion coefficients for the increasing OD band

The diffusion coefficient for both films was determined in order to elucidate the influence of the film surface on the

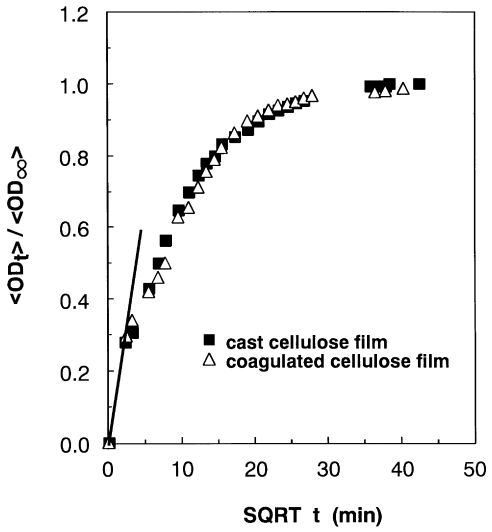

Fig. 5. The relationship between the increasing ratio of OD groups, $\langle OD_t \rangle / \langle OD_\infty \rangle$ and the square root of time (in minutes) during the deuteration process for a cast (square) and a coagulated (triangle) cellulose film. The straight line represents the slope for the two curves during the first 5 min of the reaction.

D_2O vapor diffusion into the films. A solution of Fick's Second Law of diffusion in a semi-infinite plane sheet [17] can be rewritten in the following form [18]

$$\langle OD_t \rangle / \langle OD_\infty \rangle = 4/L \cdot (D_{od} t/\pi)^{1/2},$$

where $\langle OD_t \rangle$ is the relative base-line optical density of the OD band for the sample treated in D_2O vapor for a certain time (t), $\langle OD_\infty \rangle$ the relative base-line optical density of the OD band for the sample at maximum deuteration by D_2O vapor, L the film thickness, and D_{od} the D_2O diffusion coefficient and t is time.

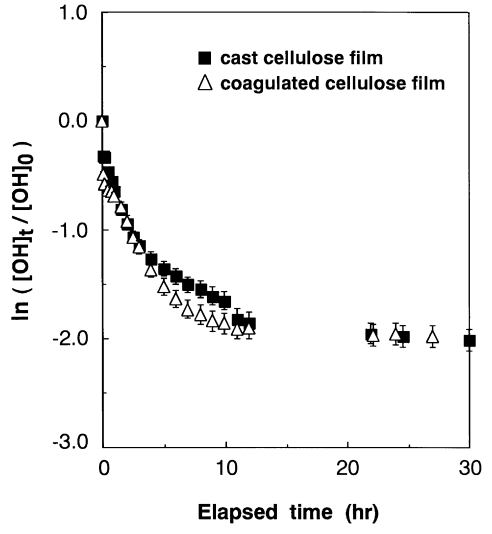

Fig. 6. The relationship between the logarithmic ratio of decreasing concentration in OH groups, $\ln \{[OH]_t/[OH]_0\}$, with time (t, hours) during the deuteration process for a cast (square) and a coagulated (triangle) cellulose film.

A plot of $\langle OD_t \rangle / \langle OD_\infty \rangle$ versus $t^{1/2}$ for each film sample yielded a curve which represents the D_2O diffusion into the film. Specifically the slope of each curve was used to calculate a D_2O diffusion coefficient for the amorphous regions in the films. Fig. 5 shows plots which were very similar to each other for both the cast and the coagulated cellulose films. The diffusion of D_2O into the amorphous regions of both films was almost totally complete in 10 h. We initially assumed that the OH–OD exchange reaction during the first 5 min could be attributed to the reaction of OH groups on the surface of the film because of the extremely rapid reduction in the OH band and corresponding increase in the OD band. We had hoped that the D_2O diffusion coefficients within the first 5 min could be used to differentiate between the two films based on their D_2O diffusion rates to penetrate the surface of the film. However, each diffusion coefficient was almost the same, 3.83×10^{-10} cm^2/min for cast cellulose film and 3.98×10^{-10} cm^2/min for coagulated cellulose film, even though the surface morphology for each film was significantly different. This suggests that the surface condition of the cellulose film, which depends on the preparation method, does not influence the D_2O diffusion rate on penetration. In addition, the rates of the deuteration as well as the D_2O diffusion rate in the amorphous regions of the cellulose films were also found to be independent of the film surface morphology at a few hundred nanometer level as described in the previous section.

3.3.2. Rate constant for the OH–OD exchange reaction

We have postulated that the OH–OD exchange reaction follows pseudo-first-order kinetics because of the presence of excess amounts of D_2O when compared to the amount of OH in each amorphous film sample [1]. Therefore, the general form for the exchange reaction can be written as:

$$-\mathrm{d}[OH]/\mathrm{d}t = k[OH], \quad (1)$$

and where Eq. (2) can be derived from Eq. (1).

$$\ln \{[OH]_t/[OH]_0\} = -kt, \quad (2)$$

where $[OH]_0$ is the initial concentration of OH (the area of the OH band) at time $t = 0$.

A plot of $\ln \{[OH]_t/[OH]_0\}$ versus time course for both cellulose films is shown in Fig. 6. It should be noted that the kinetic behavior for both plots is not a straight line but a significant curve. Although the exchange reaction in the amorphous regions of both films proceeded continuously for over 20 h, it appeared to be almost completed in 10 h when the D_2O diffusion in the amorphous regions of both films was over as described earlier (Fig. 5). The OH–OD exchange rate has been reported to depend on the diffusion of D_2O among β-glucan molecules in the cellulose sample, which means that the deuteration time for OH groups is virtually identical to the diffusion time for D_2O as the reaction was rapid enough [18]. A gradual exchange reaction continues even after 10 h due to the existence of hydrogen-bonded domains [13] in the amorphous regions which the

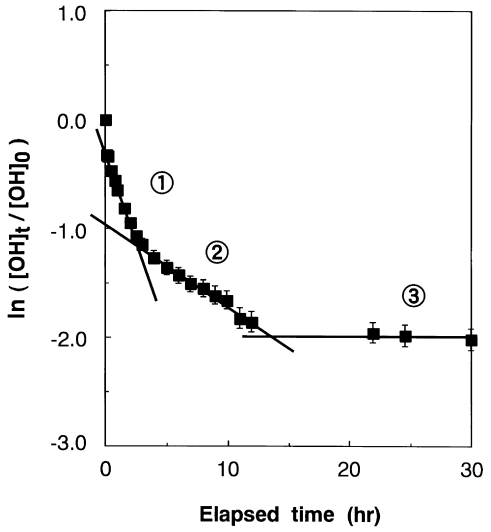

Fig. 7. The kinetic behavior for a cast cellulose film separated into three distinct single reactions. The three solid lines on the plot represent a calculated regressed fit of the points.

D_2O vapor cannot penetrate easily. Thus, we conclude that the exchange reaction rate corresponds almost identically to the diffusion rate of D_2O. Further, the reaction rate and the diffusion rate may reflect the nature of the amorphous regions in cellulose. The kinetic behavior for both films can be explained by postulating that the hydrogen-bonded domains in the amorphous regions determine the two rates during the deuteration process.

The plot of ln $\{[OH]_t/[OH]_0\}$ versus time course shown in Fig.7 was a smooth curve. As we have postulated in this study the OH–OD exchange reaction process by D_2O as a pseudo-first-order kinetics, already described, the plot should give or approximate only a straight line if the change depends on a single reaction. Therefore, the smooth curve could be deconvoluted into a sum of straight lines. As a result, the kinetic behavior for cast film was divided into three distinct single reactions (Fig. 7). Each single reaction (No. 1–3 in Fig. 7) is supposed to proceed simultaneously and competitively. This indicates that there are at least three types of domains present in amorphous regions of cast cellulose film. Reaction No. 3 in Fig. 7, which is very slow, possibly represents those domains which include unexchangeable OH groups in the amorphous film as outlined in the previous section. As for coagulated film, the nature of the amorphous regions is definitely different from that of cast film. The kinetic behavior can be divided into more than three regions as shown in Fig. 6. As the coagulation of cellulosic solution to prepare films may induce re-crystallization, we should be careful to discuss in the similar way. This behavior will be elaborated on in a future article. It should, however, be noted that the reaction rate from 15 to 60 min for coagulated film was very significantly slower than that for cast film (Fig. 8).

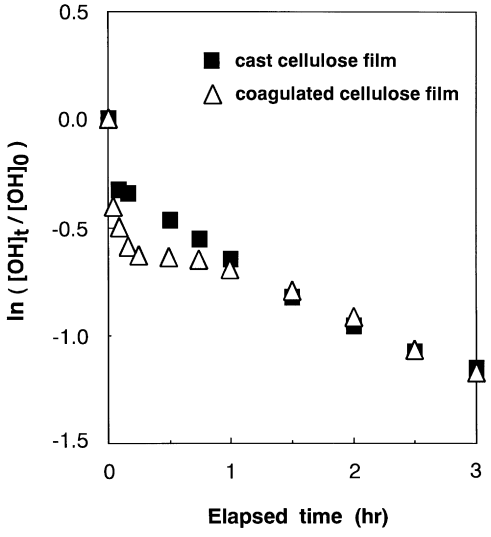

Fig. 8. The kinetic behaviors (from 0 to 3 h) for a cast (square) and a coagulated (triangle) cellulose film.

These kinetic analyses based on the reduction of the OH band revealed that the amorphous regions of cellulose films are not composed only of homogeneous domains at an IR spectroscopic level [1]. As reported previously [13], intermolecular hydrogen bonds may play an important role in the bundling of β-glucan molecules in the amorphous regions, which results in at least three types of domains as described previously. The characteristics of the domains seem to depend on the manner of cellulose film preparation.

3.4. Characterization of amorphous domains in other cellulosic materials

We have also characterized the amorphous domains in other cellulosic materials using the FTIR deuteration monitoring analysis. Two regioselectively substituted methylcellulose compounds, 2,3-di-*O*-methylcellulose (23MC) and 6-*O*-methylcellulose (6MC), were used as cellulose model systems as the hydrogen bonding in these compounds has been clarified in previous articles [19–21]. In these articles, 23MC was reported to contain intermolecular hydrogen bonds and one particular type of intramolecular hydrogen bond which forms between adjacent glucoside rings, 6MC however, is composed of only two types of intramolecular hydrogen bonds as illustrated in Fig. 9. Amorphous films of 23MC and 6MC were prepared by casting as reported previously [13,22]. The film thickness was adjusted to 17 μm for 23MC and 7 μm for 6MC, respectively. Then, each film was deuterated using D_2O vapor while monitoring the deuteration process using FTIR and kinetic analyses were carried out on the reduction of the OH band as outlined earlier.

The deuteration behavior was very similar to that of pure cellulose film in terms of the OH–OD exchange [1]. When the reaction reached an equilibrium, the amount of unexchangeable OH groups was 10.0% for the 23MC film and

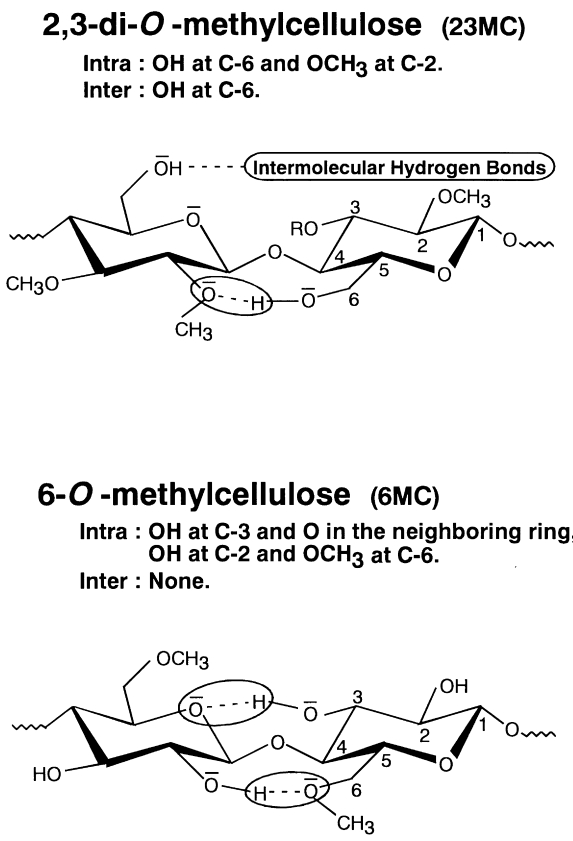

Fig. 9. The chemical structures for two regioselectively substituted methylcellulose compounds, 23MC and 6MC, and their proposed forms of hydrogen bonding.

12.6% for the 6MC film, respectively, which was very reminiscent of the results obtained for cast amorphous cellulose film. The results were also analyzed kinetically in the same manner as for cast cellulose film. The relationship between the logarithm of the decreasing ratio of OH groups, $\ln\{[OH]_t/[OH]_0\}$ and the time (t) during the deuteration process for 23MC and 6MC showed similar kinetic behavior as for cast cellulose film [1]. Namely, the results could be divided into three distinct single reactions as already described in the previous section (Section 3.2). The three rate constants indicated that both 23MC and 6MC contain at least three types of different amorphous domains.

The rate constants for the three regions of amorphous cellulosic film samples were found to be in the following order; reaction No. 1 > reaction No. 2 > reaction No. 3 (almost undeuteration), which are illustrated in Fig. 7. The aforementioned order results correspond to an assembly state of β-glucan molecules which are (i) gathered relatively loose, causing fast deuteration (reaction No. 1), (ii) packed more tightly, causing a slower deuteration (reaction No. 2) than reaction No. 1 and (iii) packed the most sturdily of the three (reaction No. 3), but not as much as for crystallites, producing the remaining unexchanged OH band. The rate constants for reaction No. 1 for the three film samples of pure cellulose, 23MC and 6MC were quite different from one another whereas those for reaction No.2 were almost identical. Table 1 shows the rate constants for reaction No.2 in the amorphous cellulosic films and the amounts of remaining OH groups after deuteration for the four samples studied. The high values for the correlation coefficients (R^2) demonstrate the consistency for the rate constant for reaction No. 2. We should add that the values for the R^2 for reaction No. 1 were also very high. It was clear that the rate constant values for reaction No. 2 for the four samples were all similar to one another. The diffusion of D_2O vapor through the films was almost completed in 10 h although the exchange reaction No. 2 continued for more than 10 h. Therefore, the reaction rate indicated the existence of the domains which were similar in character in the amorphous regions of the four film samples. Moreover in Table 1, the presence of unreacted OH groups in the amorphous 6MC film was also recognized. This may partly be due to the particular strong two types of intramolecular hydrogen bonds found in 6MC which result in poorly crystallized samples [23]. In other words, the van der Waals forces in 6MC may possibly form amorphous domains. In addition, it is interesting to note that the deuteration behavior in reaction No. 2 for 6MC is similar to that of cellulose and 23MC which commonly involve intermolecular hydrogen bonds at the C-6 position. Further investigation will be needed to clarify these observations.

4. Conclusion

The application of a FTIR deuteration monitoring analysis to examine the amorphous regions of cellulosic films

Table 1
Rate constants (k) for the OH–OD exchange reaction No. 2 in the deuteration process for three cast amorphous film samples of 23MC, 6MC and pure cellulose, and for a coagulated pure cellulose film sample, and the amounts of OH remaining after deuteration for the four samples. R^2 represents the correlation coefficient for the points

	Elapsed time (h)	$k(h^{-1})$	R^2	Percentage of OH remaining
Cast 23MC	6–12	0.085	0.97	10.0
Cast 6MC	5–13	0.057	0.99	12.6
Cast cellulose	3–12	0.075	0.98	13.3
Coagulated cellulose	5–7	0.063	1.00	
Coagulated cellulose (k_3)[a]	8–11	0.041	0.98	12.7

[a] Also concluded is the rate constant (k_3) for reaction No. 3.

showed the existence of at least three distinct rate constants for the cellulosic materials. This leads directly to the conclusion that the amorphous regions of cellulosic materials are not composed only of homogeneous domains, but of at least three different types of domains at the IR spectroscopic level. Amorphous cellulosic film samples of 23MC and 6MC prepared by a casting method also showed at least three distinct types of amorphous domains whereas coagulated cellulose films exhibited more than three domains. Moreover, it was demonstrated that some domains in each sample consisted of unreacted OH groups and we also found that some common domains exist in both cast and coagulated cellulosic films. Thus, the FTIR deuteration monitoring analysis can provide information on the, so far, unexplored nature of the amorphous regions of cellulose. Based on the aforementioned results, we want to emphasize that the combination of vapor phase deuteration and FTIR spectroscopy followed by a subsequent kinetic analysis of the reaction rates can be a very powerful tool to help characterize the nature of amorphous domains in cellulosic films.

Acknowledgements

The authors thank Dr. R.S. Werbowyj of the Pulp and Paper Research Institute of Canada (PAPRICAN) for editing the text.

References

[1] Kondo T, Kataoka Y, Hishikawa Y. ACS Symp Sers 1998;688:173.
[2] Rowland SP, Howley PS. Text Res J 1988;58:96.
[3] Mann J. In: Bikales NM, Segal L, editors. High polymers: cellulose and cellulose derivatives, part IV, 5. New York: Wiley, 1971. p. 89.
[4] Mann J, Marrinan HJ. Trans Faraday Soc 1956;52:481.
[5] Mann J, Marrinan HJ. Trans Faraday Soc 1956;52:487.
[6] Mann J, Marrinan HJ. Trans Faraday Soc 1956;52:492.
[7] Jeffries R. Polymer 1963;4:375.
[8] Taniguchi T, Harada H, Nakato K. Mokuzai Gakkaishi 1966;12:215.
[9] Marrinan HJ, Mann J. J Appl Chem 1954;4:204.
[10] Marrinan HJ, Mann J. J Polym Sci 1956;21:301.
[11] Mann J, Marrinan HJ. J Polym Sci 1958;32:357.
[12] McCormick CL, Callais PA, Hutchinson Jr BH. Macromolecules 1985;18:2394.
[13] Kondo T, Sawatari C. Polymer 1996;37:393.
[14] Togawa E, Kondo T. J Polym Sci: Part B: Polym Phys 1999;37:451.
[15] Wadehra IL, Manley RSt-J. J Appl Polym Sci 1965;9:2627.
[16] Jeffries R. J Appl Polym Sci 1968;12:425.
[17] Newns AC. Trans Faraday Soc 1956;52:1533.
[18] Hatakeyama H, Hatakeyama T. Makromol Chem 1981;182:1655.
[19] Kondo T. J Polym Sci: Part B: Polym Phys 1994;32:1229.
[20] Kondo T. Cellulose 1997;4:281.
[21] Shin J-H, Kondo T. Polymer 1998;39:6899.
[22] Kondo T, Sawatari C, Manley RSt-J, Gray DG. Macromolecules 1994;27:210.
[23] Kondo T. J Polym Sci: Part B: Polym Phys 1997;35:717.